Status and prospects of charm physics: a few considerations

S. Malvezzi[1)]

1. INFN, Milano, Italy

Abstract — The goals of quark flavor physics are to test the consistency of the Standard Model (SM) description of quark mixing and CP violation, to search for evidence of New Physics, and to select between New Physics scenarios that might be initially uncovered at the LHC. This will require a range of measurements at the percent level or better in the flavor-changing sector of the SM. Charm represents a unique candidate for these studies. Progress in charm physics has been prodigious over the last twenty years; it comes both from fixed-target and collider (e^+e^- and $p\bar{p}$) experiments, and can guide us toward future investigations. To fully exploit the potentiality of flavor physics in indicating New Physics, non-perturbative strong-interaction dynamics has to be dealt with. Complications in the determination of CP phases due to strong final-state interaction (FSI) have been uncovered; studies of charm-meson decays, mainly through Dalitz-plot analyses, have experimentally confirmed the relevance of FSI phases. Analogously, determination of Cabibbo-suppressed CKM matrix elements and $D\bar{D}$ mixing parameters will require an understanding of strong-interaction effects among the light hadrons produced in heavy-meson decays. The same complications will affect the beauty sector and will need to be kept under control to search for New Physics effects. The role of charm in the search for New Physics, the lessons learnt so far and warnings for the future will be discussed.

1 Beyond the Standard Model; the clue from charm

The success of the Standard Model in describing the experimental information to date suggests that possible deviations have to be pursued either at high-energy scales or as small effects in low-energy variables. In the Standard Model, CP violation (CPV) and flavor-changing neutral currents (FCNC) are expected to be small in charm decay, while lepton-family number violation and lepton-number violation are forbidden. Anomalously large rates for rare decays would imply non-Standard Model tree-level FCNC diagrams or non-Standard Model contributions to higher-order loop diagrams, which make them sensitive to high-mass gauge bosons and fermions and allow for probing particle states and mass scales not directly accessible [1]. The study of FCNC has been mainly dedicated to transitions such as $s \to dl^+l^-$, $s \to d\nu\bar{\nu}$, $b \to s\gamma$ and $b \to sl^+l^-$, as well as phenomena such as K^0–$\bar{K}^0$ and B^0–$\bar{B}^0$ mixing. The analogous FCNC processes in the charm sector have been investigated less. The Standard-Model expectations for both D^0–$\bar{D}^0$ mixing and FCNC are very small, while extensions of the Standard Model may enhance the contributions, which can then be orders of magnitude larger. In the Standard Model, the D system is not as sensitive to CP as the K and B mesons. In this case too, the small predicted effects could leave open a window to the observation of New-Physics effects. Charm decays may be the only window onto such New Physics since it is possible that the mechanism responsible will only couple to up-type quarks. More specifically, non-Standard-Model forces might exhibit very different patterns for the up and down classes of quarks [2]. Charm decays are the only up-type decays that afford a probe of such physics: non-strange light-flavor hadrons do not allow for oscillations and top-flavored hadrons do not even form in a practical way. In Table 1 experiments that have already published results on charm mixing, rare decays and CPV searches are listed, along with their characteristics and a reference sample. In Table 2 the expected data sets for existing experiments and proposed facilities are reported [3].

Table 1: A comparison of the LEP experiments, CDF, E791, FOCUS, CLEO, BaBar and Belle. $K^-\pi^+$ is the number of reconstructed $D^0 \to K^-\pi^+$ used in the published measurements. σ_t denotes the proper time resolution for charm hadrons.

	Fixed Target			e^+e^-		$p\bar{p}$
	E791	FOCUS	LEP	CLEO	BaBar/Belle	CDF
Beam	Hadron	Photon	$e^+e^- \to Z^0$	e^+e^-	e^+e^-	$p\bar{p}$
$K^-\pi^+$	$\sim 2\times10^4$	$\sim 2\times10^5$	$\sim 10^4$/expt.	$\sim 2\times10^5$	$\sim 10^6$	$\sim 5\times10^5$
σ_t	~ 40 fs	~ 40 fs	~ 100 fs	~ 140	~ 160 fs	~ 50 fs

Table 2: Expected $D^0 \to K^-\pi^+$ samples for the existing experiments and proposed facilities. $K^-\pi^+$ is the number of of reconstructed $D^0 \to K^-\pi^+$ in the full data set.

Experiment	Full data set	$K^-\pi^+$ reconstructed
BaBar	500 fb^{-1}	6.6×10^6
Belle	500 fb^{-1}	6.6×10^6
CDF	4.4 fb^{-1}	30×10^6
CLEO-c	3.0 fb^{-1}	5.5×10^5
BES III	30.0 fb^{-1}	5.5×10^6
BTeV		$\sim 6\times10^8/10^7$
SuperBaBar	10.0 ab^{-1}	$1.3\times10^8/10^7$ s
SuperKEKB	2.0 ab^{-1}	$2.5\times10^7/10^7$ s

1.1 Mixing

$D^0 - \bar{D}^0$ mixing in the Standard Model occurs because the two eigenstates D^0 and $\bar{D}^0$ are not mass eigenstates. The probability that a D^0 meson produced at $t = 0$ decays as a $\bar{D}^0$ at time t is given by

$$P(D^0 \to \bar{D}^0) = \frac{1}{4}e^{-\Gamma_1 t}\left\{1 - 2e^{\frac{-\Delta\Gamma}{2}}\cos\Delta m t + e^{-\Delta\Gamma t}\right\} \quad (1)$$

where $\Delta m = m_2 - m_1$, $\Delta\Gamma = \Gamma_2 - \Gamma_1$ are the mass and width differences of the mass eigenstates and $\Gamma = \frac{\Gamma_1+\Gamma_2}{2}$. In the limit $\Delta m, \Delta\Gamma << \Gamma$, mixing effects are parametrized by two dimensionless amplitudes $x = \frac{\Delta m}{\Gamma}$ and $y = \frac{\Delta\Gamma}{2\Gamma}$. The experimental measurement is performed by analyzing wrong sign semileptonic and hadronic decays; the presence of doubly Cabibbo-suppressed decays complicates the measurement in the hadronic sector. Assuming CP conservation, the wrong sign to right sign decay rate is

$$r_D(t) = e^{-\Gamma t}\left(R_{DCS} + \sqrt{R_{DCS}}\,y'\Gamma t + \frac{1}{4}(x'^2 + y'^2)\Gamma^2 t^2\right) \quad (2)$$

where $y' = y\cos\delta - x\sin\delta$ and $x' = x\cos\delta + y\sin\delta$, δ being the strong phase difference between the Cabibbo-favored and Doubly Cabibbo-suppressed Decay (DCS). The three terms come from DCS decays, interference, and mixing. In the semileptonic mixing only the last term matters. The up-to-date experimental situation is summarized in Fig. 1 [4, 5]. In the semileptonic sector, FOCUS has measured, preliminarily, r_D in the mode $D^0 \to K^+\mu^-\bar{\nu}_\mu$ to be less than 0.131% @ 95% C.L.; CLEO-c expects r_D less than 10^{-4}% @ 95% C.L.; SuperBaBar estimates that, with 10 ab^{-1}, the sensitivity would be $r_D < 5\times10^{-4}$. With 10^9 reconstructed charm decays BTeV expects to reach a sensitivity of 1–2 $\times 10^{-5}$. An observation of mixing at the level of $10^{-4} - 10^{-5}$, which could be probed by a high-sensitivity experiment, would be a signal of New Physics. In Fig. 1 measurements of the lifetime difference between D^0 decays to CP-even and CP-odd final states are also shown. If CP violation in neutral D-meson decays is negligible we can write

$$y_{CP} = \frac{\Gamma(\text{CP even}) - \Gamma(\text{CP odd})}{\Gamma(\text{CP even}) + \Gamma(\text{CP odd})} \sim \frac{\Gamma(D^0 \to K^+K^-)}{\Gamma(D^0 \to K^-\pi^+)} - 1 \quad (3)$$

The theoretical prediction spread of the mixing parameters is wild, as shown in the right side of Fig. 1; independently of New Physics discovery, accurate experimental measurements are necessary.

1.2 CP Violation

CP violation can occur in charm decays via the interference of two weak decay amplitudes to the same final state. *Indirect* CP violation is mediated by D^0–$\bar{D}^0$ mixing. The interference is the largest if the two amplitudes

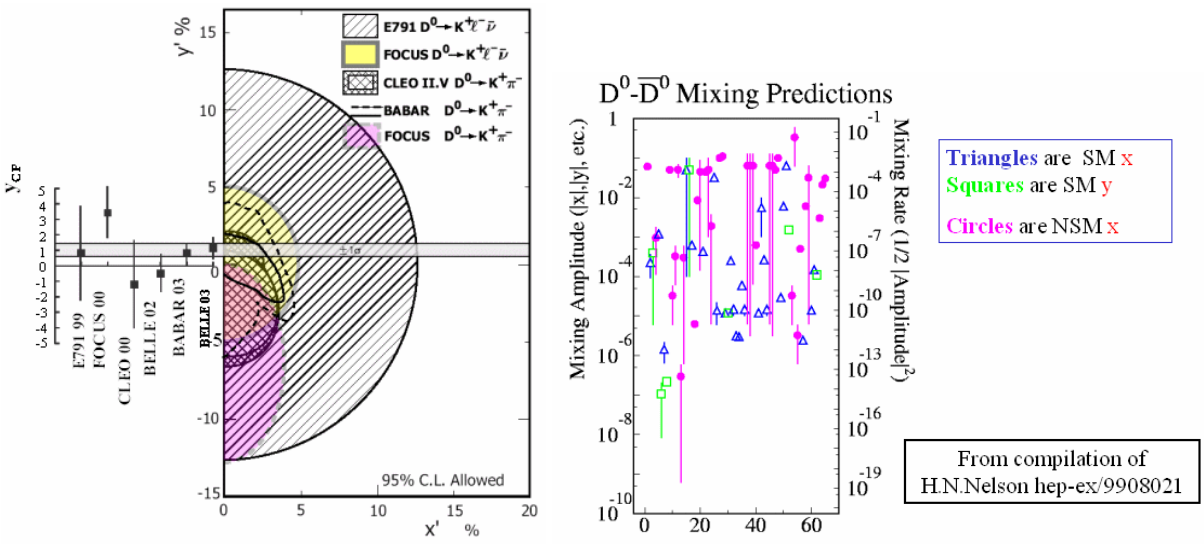

Figure 1: Mixing scenario.

are roughly equal. However, since mixing is expected to be small, indirect CP violation is not expected to be a big effect. In absence of mixing, a decay mode (e.g., a Cabibbo-suppressed decay) that has two weak amplitudes contributing to the same final state can exhibit *direct* CP violation. Final State Interactions (FSI) can induce a phase shift between the two weak amplitudes, leading to a decay-rate asymmetry between a charm meson decay and its CP conjugate: $\Gamma(D \to f) \neq \Gamma(\bar{D} \to \bar{f})$. FSI are substantial in charm decay, and the two weak amplitudes can be similar in size. Asymmetries as large as 0.1–1% are possible in the Standard Model. In Table 3 the experimental scenario is reported.

Table 3: Measurements of CP asymmetries.

Decay mode	E791	CLEO
$D^0 \to K^-K^+$	$-0.010 \pm 0.049 \pm 0.012$	$0.000 \pm 0.022 \pm 0.008$
$D^0 \to \pi^-\pi^+$	$-0.049 \pm 0.078 \pm 0.030$	$0.030 \pm 0.032 \pm 0.008$
$D^0 \to K_sK_s$		-0.23 ± 0.19
$D^0 \to K_s\pi^0$		0.001 ± 0.013
$D^0 \to \pi^0\pi^0$		0.001 ± 0.048
$D^+ \to K^-K^+\pi^+$	-0.014 ± 0.029	
$D^+ \to \pi^-\pi^+\pi^+$	-0.017 ± 0.042	
	FOCUS	CDF
$D^0 \to K^-K^+$	$-0.001 \pm 0.022 \pm 0.015$	$0.020 \pm 0.012 \pm 0.006$
$D^0 \to \pi^-\pi^+$	$0.048 \pm 0.039 \pm 0.025$	$0.030 \pm 0.013 \pm 0.006$
$D^+ \to K^-K^+\pi^+$	$0.006 \pm 0.011 \pm 0.005$	
$D^+ \to K_s\pi^+$	$-0.016 \pm 0.015 \pm 0.009$	
$D^+ \to K_sK^+$	$0.071 \pm 0.061 \pm 0.012$	

Expectations come from CLEO-c, which aims at exploiting the quantum coherence of the D^0–$\bar{D}^0$ pair produced. The process $e^+e^- \to \psi'' \to D^0\bar{D}^0$ produces a CP+ eigenstate in the first step, since ψ'' has $J^{PC} = 1^{--}$. Consider the case where both the D^0 and the $\bar{D}^0$ decay into CP eigenstates. Then the decays $\psi'' \to f_+^i f_+^i$ or $f_-^i f_-^i$ are forbidden, where f_+/f_- denotes a CP+ / CP- eigenstates. This is because $CP(f_\pm^i f_\pm^i) = (-1)^l = -1$ for the l=1 ψ''. Thus, observation of a final state such as $(K^+K^-)(\pi^+\pi^-)$ constitutes evidence of CP violation. Of course this method requires a complete understanding of the Initial State Radiation (ISR) effects. CP asymmetries measured so far in the charm sector are consistent with zero within the errors. The high statistics soon available from experiments such as Belle, BaBar and CLEO-c would be able to probe CP asymmetries at the 10^{-3} level. BTeV and will extend the sensitivity below the 10^{-3} level.

1.2.1 CP investigation via Dalitz-plot analysis

Dalitz-plot analysis has recently emerged as a unique tool to investigate CPV effects. Amplitude analysis gives the full observation of a three-body decay, providing access to the coefficients and phases of the various channels. CP effects are intimately connected to phase phenomena. The comparison between the relative phases of the CP-conjugate states for the various resonant channels can address CPV effects. FOCUS analyzed the $D^+ \to K^-K^+\pi^+$ channel [6] and CLEO the $D^0 \to K_S\pi^+\pi^-$ channel [7]. In general each measured phase in the Dalitz plot can be interpreted as a sum of two components, one CP conserving, the other CP violating. Under CP conjugation the first does not switch sign, while the second does. The $D^+ \to K^-K^+\pi^+$ channel is a good candidate to observe CP effects. This decay is Cabibbo suppressed and thus contains two diagrams contributing to the final state, spectators and penguins; it is also dominated by strong effects, as discussed above, and thus satisfies the two necessary requirements for detecting a CP asymmetry. FOCUS [6] has performed a new Dalitz-plot study, which proceeds through a complete Dalitz analysis of the D^+/D^- split samples. The preliminary results on D^+/D^- coefficients and phases, shown in Fig. 2, do not point to any CPV manifestation. The relative phases are measured with an accuracy of about 5–10°. The errors are affected by a large correlation among the various resonant components necessary to fit the Dalitz plot. A more robust formalism, such as the *K-matrix* approach, which will be discussed later in this paper, might allow for a good fit with fewer resonances, thus ameliorating the accuracy of the phase measurements. At any rate a factor of 100 more statistics, as hopefully available in BTeV, will allow for reaching sensitivities of a degree.

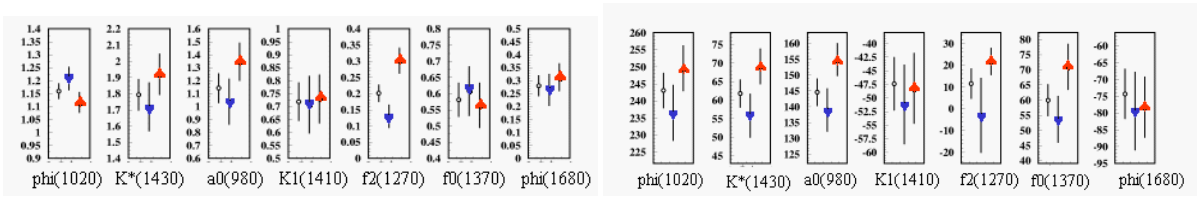

Figure 2: Amplitude coefficient and relative phases (in degrees) of all the resonant contributions of the $D^+ \to K^-K^+\pi^+$ decay: the circles are for the full sample, upward triangles for D^- and downward triangles for D^+.

1.3 Rare decays

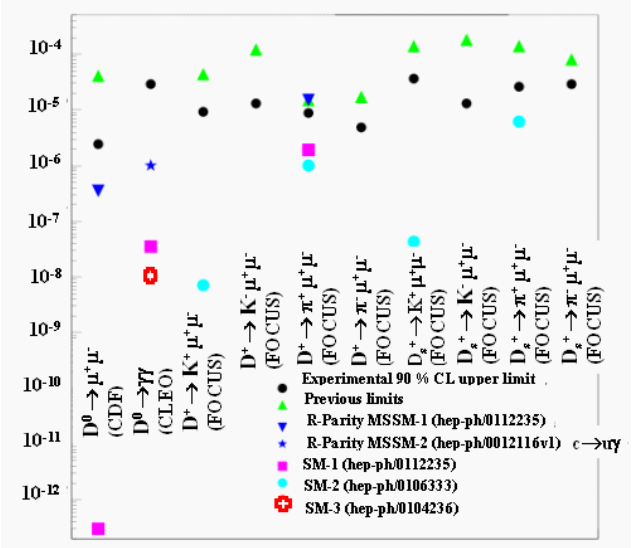

Figure 3: Measurements of rare decays.

The search for rare and forbidden decays is enticing since Standard Model predictions tend to be beyond the reach of current experiments, and a signal is a sign of unexpected physics. Standard Model predictions of rare decays are dominated by long-range effects, which are notoriously difficult to calculate and experimental measurements are thus crucial. The current experimental scenario concerning rare decay branching ratios is reported in Fig. 3. FOCUS [8] has improved many of the previous limits of a factor from 2 to 14. The strength of the FOCUS fixed target experiment is the excellent vertexing, which was used to require that the two candidate leptons form a good, well separated vertex from the primary. CDF and D0 have efficient di-lepton triggers and future measurements are

promising. The reported CDF result is obtained only with a statistics of $65\,\mathrm{pb}^{-1}$. A new limit of 2×10^{-6} has been recently provided by the Hera-B experiment[9]. CLEO-c sensitivity is estimated at the level of 10^{-6}.

2 Standard Model measurements and lessons for the future

The variety of measurements above briefly discussed represents an excellent opportunity for searching New Physics in the charm sector. Effects beyond the Standard Model are, as already pointed out, expected to be small, making their investigations really challenging. Possible tiny inconsistencies and deviations from expected behavior can be interpreted as sign of New Physics only if the Standard Model phenomenology is correctly parametrized in the analysis procedure. The main lesson coming from the mature field of charm is that the advantages of high statistics to interpret the Heavy Flavor decay dynamics will vanish in the absence of a strategy to control strong effects among particles involved in weak decay processes. A few examples from the FOCUS experiment will be discussed.

2.1 Unexpected new results in the semileptonic sector

Semileptonic decays have always been considered the best candidates to study the charm phenomenology. Decay rates can be calculated from first principles, e.g, Feynman diagrams; due to the presence of only one hadron in the final state we do not have to worry much about final state interaction complications; the hadronic part of the decay can be contained in proper form factors, which, on their turn can be predicted by theory such as HQET, LGT and Quark models. However recent FOCUS studies have shown that decays in the semileptonic sector also reveal the presence of quantum mechanical effects and hadronic complications have to be dealt with in the analysis. Of particular relevance is the study of $D^+ \to K^-\pi^+\mu^+\nu$ [10]. The FOCUS mass spectrum appears, as expected, dominated by $\bar{K}^{*0}(892)$; yet an unexpected forward-backward asymmetry was exposed in the $\cos\theta_V$ variable, defined in Fig. 4. The asymmetry is striking below the pole and essentially absent above the pole: it thus suggests quantum-mechanical interference between the Breit–Wigner amplitude describing the $\bar{K}^{*0}(892)$ and a broad or nearly constant S-wave amplitude. FOCUS has tried to describe this behavior of the decay distribution for $D^+ \to K^-\pi^+\mu^+\nu$ through a simple model. It has been written in terms of the three helicity-basis form factors: H_+, H_0, H_-, and the S-wave amplitude modeled as a constant, with modulus A and phase δ has been added. Angular momentum conservation restricts the S-wave contribution to the H_0 piece that describes the amplitude for having the virtual W^+ in a zero helicity state relative to its momentum vector in the D^+ rest-frame.

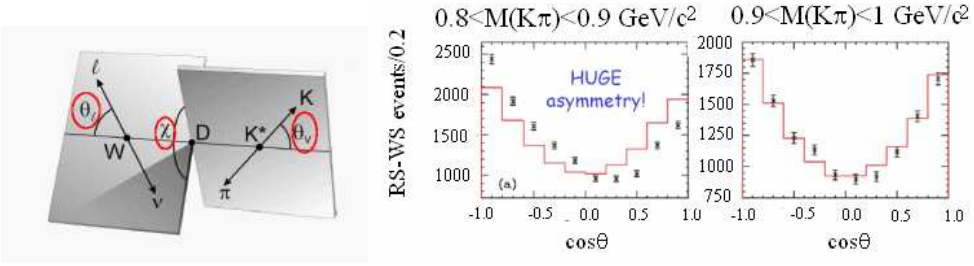

Figure 4: The definition of the kinematic variables for the $D^+ \to \bar{K}^{*0}\mu^+\nu$ and $\cos\theta_V$ distribution.

The shape of the $\cos\theta_V$ term versus $m_{K\pi}$ turns out to be a strong function of the interfering S-wave amplitude phase δ. Figure 5 shows how the $\cos\theta_V$ distribution (properly weighted) is consistent with a constant S-wave amplitude of the form $0.36\exp(i\pi/4)\,(\mathrm{GeV})^{-1}$, although, at this stage of the analysis, the solution is not unique; alternative modelings of the S-wave amplitude, as shown in the same Fig. 5, could also fit the data. The measured phase of $\pi/4$ is consistent with that found by LASS from the $K\pi$ phase-shift analysis. The hypothesis of the broad scalar resonance κ is disfavored since it would imply a phase-shift of approximately 90° with respect to $\bar{K}^{*0}(892)$, unlikely to manifest in the semileptonic sector where FSI are not expected to be wild [11]. A more precise determination can be obtained through a complete analysis of the form factor ratios r_v and r_2 [12]. FOCUS has found $r_v = 1.504 \pm 0.057 \pm 0.039$ and $r_2 = 0.875 \pm 0.049 \pm 0.064$. For the S-wave we obtained an amplitude modulus of $A = 0.330 \pm 0.022 \pm 0.015\,\mathrm{GeV}^{-1}$ and a phase $\delta = 0.68 \pm 0.07 \pm 0.05$ rad, in reasonable agreement with the very informal previous estimate of $A = 0.36\exp(i\pi/4)\,\mathrm{GeV}^{-1}$. The inclusion of the S-wave amplitude has dramatically improved the quality of the form factor fits. A measurement of the branching ratio $\frac{\Gamma(D^+\to\bar{K}^{*0}\mu^+\nu)}{\Gamma(D^+\to K^-\pi^+\pi^+)} = 0.602 \pm 0.01(\mathrm{stat.}) \pm 0.021(\mathrm{syst.})$ has then been performed including interference with this broad scalar resonance. To complete the semileptonic study, FOCUS has performed an analysis of the $D_s^+ \to$

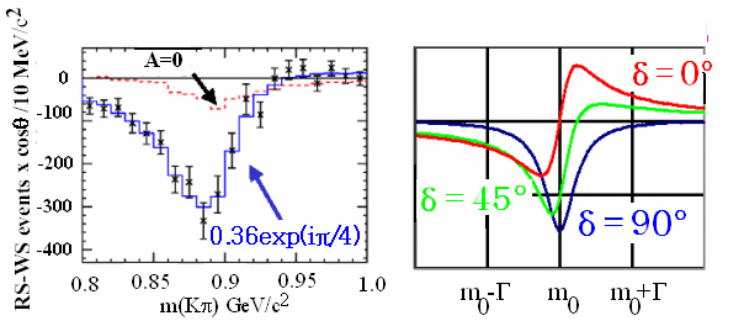

Figure 5: Asymmetry distribution in $K\pi$ invariant mass. The dashed line is the MC with no S-wave amplitude, the solid line is the MC with an S-wave amplitude of $0.36\exp(i\pi/4)\,(\mathrm{GeV})^{-1}$. Different modelings of the S-wave are also shown.

$\phi\mu^+\nu$ final state; the $\frac{\Gamma(D_s^+\to\phi\mu^+\nu)}{\Gamma(D_s^+\to\phi\pi^+)}$ has been measured to be $0.54 \pm 0.033(\mathrm{stat.}) \pm 0.048(\mathrm{syst.})$ [13], and a new measurement of form factor ratios has been recently published [14].

2.2 Unexpected complications in hadronic decay dynamics: D^+ and $D_s^+ \to \pi^+\pi^-\pi^+$

Charm-meson decay dynamics has been extensively studied in the last decade. The analysis of the three-body final state by fitting Dalitz plots has proved to be a powerful tool for investigating effects of resonant substructure, interference patterns, and final state interactions in the charm sector. An example of Dalitz-plot analysis to study CP-violation effects has been already discussed in a section of this paper. The isobar formalism, which has traditionally been applied to charm amplitude analyses, represents the decay amplitude as a sum of relativistic Breit–Wigner propagators multiplied by form factors plus a term describing the angular distribution of the two body decay of each intermediate state of a given spin. Many amplitude analyses require detailed knowledge of the light-meson sector. In particular, the need to model intermediate scalar particles contributing to the charm meson decays into three-body hadronic channels has caused experimentalists of the field to question the validity of the Breit–Wigner approximation for the description of the relevant scalar resonances [15, 16, 17]. Resonances are associated with poles of the *S-matrix* in the complex energy plane. The position of the pole in the complex energy plane provides the fundamental, model-independent, process-independent resonance description. A simple Breit–Wigner amplitude corresponds to the most elementary type of extrapolation from the physical region to an unphysical-sheet pole. In the case of a narrow, isolated resonance, there is a close connection between the position of the pole on the unphysical sheet and the peak we observe in experiments at real values of the energy. However, when a resonance is broad and overlaps with other resonances, then this connection is lost. The Breit–Wigner parameters measured on the real axis (mass and width) can be connected to the pole-positions in the complex energy plane only through models of analytic continuation. A formalism for studying overlapping and many channel resonances has been proposed long ago and is based on the *K-matrix* [18, 19] parametrization. This formalism, originating in the context of two-body scattering, can be generalized to cover the case of production of resonances in more complex reactions [20], with the assumption that the two-body system in the final state is an isolated one and that the two particles do not simultaneously interact with the rest of the final state in the production process [19]. The *K-matrix* approach allows for including the positions of the poles in the complex plane directly in the analysis, incorporating in the charm analysis the results from light spectroscopy experiments [21, 22]. In addition, the *K-matrix* formalism provides a direct way of imposing the two-body unitarity constraint which is not explicitly guaranteed in the simple isobar model. Minor unitarity violations are expected for narrow, isolated resonances but more severe ones exist for broad, overlapping states. The validity of the assumed quasi two-body nature of the process of the *K-matrix* approach can only be verified by a direct comparison of the model predictions with data. In particular, the failure to reproduce three-body-decay features would be a strong indication of the presence of neglected three-body effects.

2.3 The isobar formalism

The formalism traditionally applied to three-body charm decays relies on the so-called isobar model. A resonant amplitude for a quasi-two-body channel, of the type

$$\begin{aligned} D \to \quad & r + c \\ & \hookrightarrow a + b\,, \end{aligned} \tag{4}$$

is interpreted *à la* Feynman. For the decay $D \to \pi\pi\pi$ of Fig. 6, a $D \to \pi$ current with form factor F_D interacts

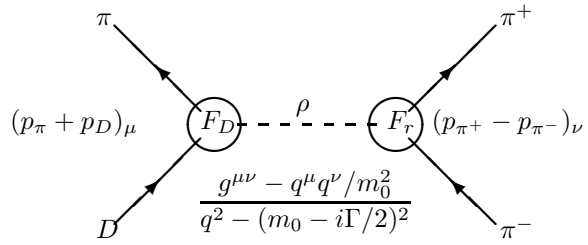

Figure 6: The $D^+ \to \pi\pi\pi$ decay diagram.

with a di-pion current with form factor F_r through an unstable propagator with an imaginary width contribution in the propagator mass. Each resonant decay function is thus,

$$A = F_D F_r \times |\vec{c}|^J |\vec{a}|^J P_J(\cos\Theta^r_{ac}) \times BW(m_{ab}) \tag{5}$$

i.e., the product of two vertex form factors (Blatt–Weisskopf momentum-dependent factors), a Legendre polynomial of order J representing the angular decay wave function, and a relativistic Breit–Wigner (BW). In this approach, already applied in the previous analyses of the same channels [23], the total amplitude (Eq. 6) is assumed to consist of a constant term describing the direct non-resonant three-body decay and a sum of functions (Eq. 5) representing intermediate two-body resonances.

$$A(D) = a_0 e^{i\delta_0} + \sum_i a_i e^{i\delta_i} A_i \,, \tag{6}$$

2.4 The *K-matrix* formalism

For a well-defined wave of specific isospin and spin *IJ*, characterized by narrow and isolated resonances the propagator is, as anticipated, of the simple BW form. In contrast, when the specific wave *IJ* is characterized by large and heavily overlapping resonances, just as the scalars, the propagation is no longer dominated by a single resonance, but is the result of complicated interplay among the various resonances. In this case, it can be demonstrated on very general grounds that the propagator may be written in the context of the *K-matrix* approach as

$$(I - iK \cdot \rho)^{-1} \tag{7}$$

where *K* is the matrix for the scattering of particle a and b (Eq. 4) and ρ is the phase-space matrix. In this picture, the production process is viewed as consisting of an initial preparation of several states, which then propagate via the term $(I - iK\rho)^{-1}$ into the final state. In particular, the three-pion final state can be fed by an initial formation of $(\pi\pi)\pi$, $(K\overline{K})\pi$, $(\eta\eta)\pi$, $(\eta\eta')\pi$ and multi-meson states (mainly four-pion states at $\sqrt{s} < 1.6\,\text{GeV}$). While the need for a *K-matrix* parametrization, or in general for a more accurate description than the isobar model, might be questionable for the vector and tensor amplitudes, since the resonances are relatively narrow and well isolated, this parametrization is needed for the correct treatment of scalar amplitudes. Indeed the $\pi\pi$ scalar resonances are large and overlap each other in such a way that it is impossible to single out the effect of any one of them on the real axis. In order to write down the propagator, we need the scattering matrix. To perform a meaningful fit to D mesons to three-pion data, a full description of the scalar resonances in the relevant energy range, updated to the most recent measurements in this sector is needed. At the present time the only self-consistent description of S-wave isoscalar scattering is that given in the *K-matrix* representation by Anisovich and Sarantsev in [22] through a global fit of the available scattering data from the $\pi\pi$ threshold up to 1900 MeV. FOCUS has performed the first fit to charm data with the *K-matrix* formalism [24] in the D^+ and $D_s^+ \to \pi^+\pi^-\pi^+$ channels. The *K-matrix* used is that of [22]:

$$K^{00}_{ij}(s) = \left\{ \sum_\alpha \frac{g_i^{(\alpha)} g_j^{(\alpha)}}{m_\alpha^2 - s} + f_{ij}^{\text{scatt}} \frac{1\,\text{GeV}^2 - s_0^{\text{scatt}}}{s - s_0^{\text{scatt}}} \right\} \times \frac{s - s_A m_\pi^2/2}{(s - s_{A0})(1 - s_{A0})}. \tag{8}$$

The factor $g_i^{(\alpha)}$ is the coupling constant of the *K-matrix* pole α to meson channel i; the parameters f_{ij}^{scatt} and s_0^{scatt} describe a smooth part of the *K-matrix* elements; the factor $\frac{s - s_A m_\pi^2/2}{(s - s_{A0})(1 - s_{A0})}$ suppresses a false kinematical singularity in the physical region near the $\pi\pi$ threshold (Adler zero). The *K-matrix* values of [22] generate a physical *T-matrix*, $T = (I - i\rho \cdot K)^{-1} K$, which describes the scattering in the $(00)^{++}$-wave with five poles, whose

masses, half-widths, in GeV are $(1.019, 0.038)$, $(1.306, 0.167)$, $(1.470, 0.960)$, $(1.489, 0.058)$ and $(1.749, 0.165)$. The *K-matrix* formalism, originated in the context of the two-body scattering, can be generalized to deal with formation of resonances in more complex reactions, through the *P-vector* [20] approach. The decay amplitude for the D meson into three-pion final state, where $\pi^+\pi^-$ are in a $(IJ^{PC} = 00^{++})$-wave, can thus written as

$$A(D \to (\pi^+\pi^-)_{00^{++}}\pi^+) = F_1 = (I - iK\rho)^{-1}_{1j}$$
$$\times \left\{ \sum_\alpha \frac{\beta_\alpha g_j^{(\alpha)}}{m_\alpha^2 - m^2} + f_{1j}^{\rm prod} \frac{1\,{\rm GeV}^2 - s_0^{\rm prod}}{s - s_0^{\rm prod}} \right\} \times \frac{s - s_A m_\pi^2/2}{(s - s_{A0})(1 - s_{A0})}. \tag{9}$$

where β_α is the coupling to the pole α in the 'initial' production process, $f_{1j}^{\rm prod}$ and $s_0^{\rm prod}$ are the *P-vector* slowly varying (SVP) parameters. In the end, the complete decay amplitude of the D meson into three-pion final state is [24]:

$$A(D) = a_0 e^{i\delta_0} + \sum_i a_i e^{i\delta_i} A_i + F_1 \tag{10}$$

where the index i now runs only over the vector and tensor resonances, which can be safely treated as simple Breit–Wigner's (see Eq. 5). In the fit to the data, the *K-matrix* parameters are fixed to the values of [22], which consistently reproduce measured S-wave isoscalar scattering. The free parameters are those peculiar to the *P-vector*, i.e., β_α, $f_{1j}^{\rm prod}$ and $s_0^{\rm prod}$, and those in the remaining isobar part of the amplitude, a_i and δ_i.

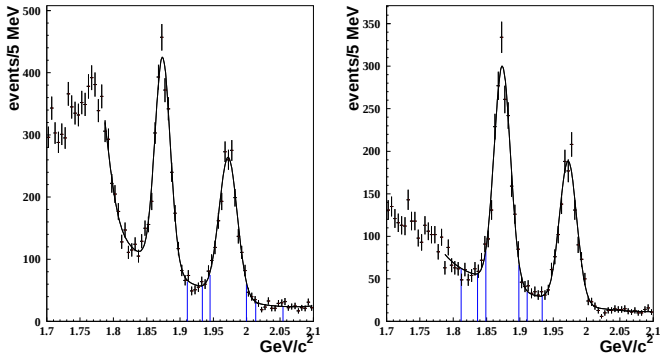

(a) D_s^+ (b) D^+

Figure 7: Signal and side-band regions of the three-pion invariant-mass distribution for a) D_s^+ and b) D^+ Dalitz-plot analysis respectively.

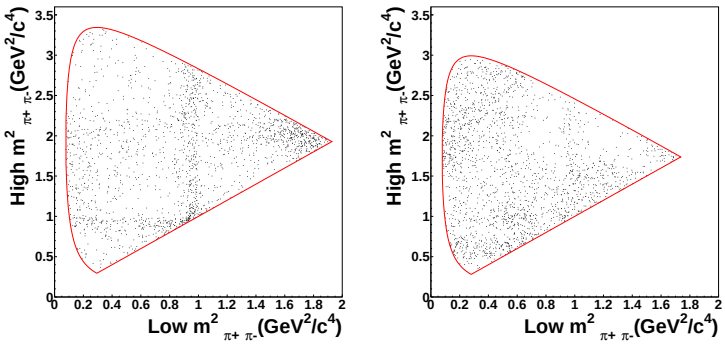

(a) D_s^+ (b) D^+

Figure 8: a) D_s^+ and b) D^+ Dalitz plots.

The three-pion selected samples (Fig. 7) consist of 1527 ± 51 and 1475 ± 50 events for the D^+ and D_s respectively. The Dalitz-plot (Fig. 8) analyses are performed on yields within $\pm 2\sigma$ of the fitted mass value.

2.4.1 Results for the $D_s^+ \to \pi^+\pi^-\pi^+$ decay

The general procedure adopted for the fits consists of several successive steps in order to eliminate contributions whose effects on fits are marginal. Initially all the well established, non-scalar resonances decaying to $\pi^+\pi^-$ with a sizeable branching ratio are considered. Contributions are removed if their amplitude coefficients, a_i of Eq. 10, are less than $2\,\sigma$ significant *and* the fit confidence level increases due to the decreased number of degrees of freedom in the fit. The *P-vector* initial form includes the complete set of *K-matrix* poles and slowly varying function (SVP) as given in reference [22]; β_α as well as the $f_{1j}^{\rm prod}$ terms of Eq. 9 are removed with the same criteria. The fit confidence levels (C.L.) are evaluated with a χ^2 estimator over a Dalitz plot with bin size adaptively chosen to maintain a minimum number of events in each bin. Once the minimal set of parameters is reached, addition of each single contribution previously eliminated is reinstated to verify that the C.L. does not improve. The resulting fit fractions [1)], phases and amplitude coefficients are quoted in Table 4. Both the three-body non-resonant and $\rho^0(770)\pi^+$ components are not required by the fit. This result is to be compared with that obtained with the simple isobar model, which requires a non-resonant component of about 25% to get a decent fit to the data [25]. This component, which crosses the Dalitz plot uniformly, seems to compensate, with its interference with the other contributions, for the inability of the model to properly describe some non-trivial resonant features not properly accounted for in the model. In this way the potentiality of the Dalitz-plot analysis to gauge the level of the annihilation contribution in the charm hadronic decays is limited. An additional difficulty with the isobar model is the general poor knowledge of scalar resonances: the measurements reported in the PDG are dispersed over a wide range of values and can not be used as input parameters of charm decay amplitudes. Masses and widths of the corresponding Breit-Wigner forms have to be let free in the fit: the isobar model can thus be viewed as an effective model able to reproduce the data with a sum of effective resonances but its phenomenological interpretation has to be considered with caution. The entire S-wave contribution obtained with the *K-matrix* formalism is represented by a single fit fraction since, as previously discussed, one cannot distinguish the different resonance or SVP S-wave contributions on the real axis. The D_s^+ Dalitz projections of FOCUS data are shown in Fig. 9 superimposed with final fit projections. The fit C.L. is 3%.

Table 4: Fit results from the *K-matrix* model for D_s^+.

decay channel	fit fraction (%)	phase (deg)	amplitude coefficient
(S-wave) π^+	$87.04 \pm 5.60 \pm 4.17$	0 (fixed)	1 (fixed)
$f_2(1270)\,\pi^+$	$9.74 \pm 4.49 \pm 2.63$	$168.0 \pm 18.7 \pm 2.5$	$0.165 \pm 0.033 \pm 0.032$
$\rho^0(1450)\,\pi^+$	$6.56 \pm 3.43 \pm 3.31$	$234.9 \pm 19.5 \pm 13.3$	$0.136 \pm 0.030 \pm 0.035$
Fit C.L	3.0%		

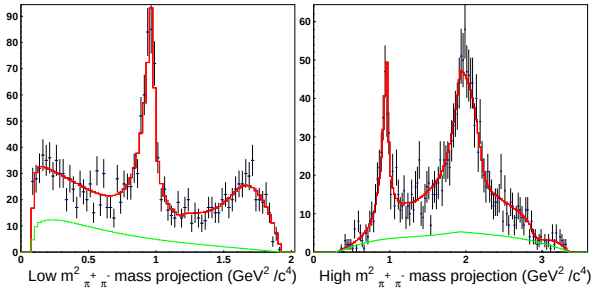

Figure 9: D_s^+ Dalitz-plot projections with the *K-matrix* fit superimposed. The background shape under the signal is also shown.

[1)] The quoted fit fractions are defined as the ratio between the intensity for a single amplitude integrated over the Dalitz plot and that of the total amplitude with all the modes and interferences present.

2.4.2 Results for the $D^+ \to \pi^+\pi^-\pi^+$ decay

The $D^+ \to \pi^+\pi^-\pi^+$ Dalitz plot shows an excess of events at low $\pi^+\pi^-$ mass, which cannot be explained in the context of the simple isobar model with the usual mixture of well established resonances along with a constant, non-resonant amplitude. A new scalar resonance, the $\sigma(600)$, has been previously proposed [26] to describe this excess. However we know that complex structure can be generated by the interplay among the S-wave resonances and the underlying non-resonant S-wave component that cannot be properly described in the context of a simple isobar model. It is therefore interesting to study this channel with the present formalism, which embeds all the experimental knowledge about the S-wave $\pi^+\pi^-$ scattering dynamics. With the same procedure based on statistical significance and fit confidence level used in the D_s^+ analysis, the final set of contributions is reached. Beside the S-wave component, the decay appears to be dominated by the $\rho^0(770)$ plus a $f_2(1270)$ component. The $\rho^0(1450)$ was always found to have less than $2\,\sigma$ significance and was therefore dropped from the final fit. In analogy with the D_s^+, the direct three-body non-resonant component was not necessary since the SVP of the S-wave could reproduce the entire non-resonant portion of the Dalitz plot. The complete fit results are reported in Table 5. The D^+ Dalitz projections are shown in Fig. 10. The fit C.L. is 7.7%.

Table 5: Fit results from the *K-matrix* model fit for D^+.

decay channel	fit fraction (%)	phase (deg)	amplitude coefficient
(S-wave) π^+	$56.00 \pm 3.24 \pm 2.08$	0 (fixed)	1 (fixed)
$f_2(1270)\,\pi^+$	$11.74 \pm 1.90 \pm 0.23$	$-47.5 \pm 18.7 \pm 11.7$	$1.147 \pm 0.291 \pm 0.047$
$\rho^0(770)\,\pi^+$	$30.82 \pm 3.14 \pm 2.29$	$-139.4 \pm 16.5 \pm 9.9$	$1.858 \pm 0.505 \pm 0.033$
Fit C.L.	7.7%		

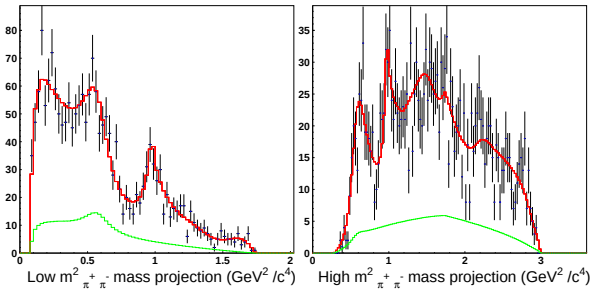

Figure 10: D^+ Dalitz-plot projections with the final fit superimposed. The background shape under the signal is also shown.

The most interesting feature of these results is the fact that the better treatment of the S-wave contribution provided by the *K-matrix* model can reproduce the low-mass $\pi^+\pi^-$ structure of the D^+ Dalitz plot. This suggests that any σ-like object in the D decay should be consistent with the same σ-like object measured in the $\pi^+\pi^-$ scattering. Additional studies with higher statistics will be required to completely understand the σ puzzle. It is interesting to recall the close analogy between the $D \to \pi\pi\pi$ channel and the $B \to \rho\pi$ one, which is a good candidate to measure the angle α of the Standard Model Unitarity Triangle; the analysis of $B \to \rho\pi$ will proceed through a time-dependent Dalitz-plot analysis of the three-pion final state and will likely present similar parametrization complications.

2.5 Interpretation of the D_s^+ and $D^+ \to \pi^+\pi^-\pi^+$ results

The *K-matrix* formalism has been applied for the first time to the charm sector in the FOCUS Dalitz-plot analyses of the D_s^+ and $D^+ \to \pi^+\pi^-\pi^+$ final states. The results are extremely encouraging since the same *K-matrix* description gives a coherent picture of both two-body scattering measurements in light-quark experiments *as well as* charm meson decay. This result was not obvious beforehand. Furthermore, the same model is able to reproduce features of the $D^+ \to \pi^+\pi^-\pi^+$ Dalitz plot that otherwise would require an *ad hoc* σ resonance. In addition, the non-resonant component of each decay seems to be described by known two-body S-wave dynamics without the need to include constant amplitude contributions. The *K-matrix* treatment of the S-wave component of the decay amplitude allows for a direct interpretation of the decay mechanism in terms of the five virtual channels considered:

$\pi\pi$, $K\bar{K}$, $\eta\eta$, $\eta\eta'$ and $4\,\pi$. By inserting KK^{-1} in the decay amplitude, F,

$$F = (I - iK\rho)^{-1}P = (I - iK\rho)^{-1}KK^{-1}P = TK^{-1}P = TQ \tag{11}$$

we can view the decay as consisting of an initial production of the five virtual states which then scatter via the physical T into the final state. The *Q-vector* contains the production amplitude of each virtual channel in the decay. The resulting picture, for both D_s^+ and D^+ decay, is that the S-wave decay is dominated by an initial production of $\eta\eta$, $\eta\eta'$ and $K\bar{K}$ states. Dipion production is always much smaller. This suggests that in both cases the S-wave decay amplitude primarily arises from a $s\bar{s}$ contribution such as that produced by the Cabibbo-favored weak diagram for the D_s^+ and one of the two possible singly Cabibbo-suppressed diagrams for the D^+. For the D^+, the $s\bar{s}$ contribution competes with a $d\bar{d}$ contribution. That the $f_0(980)$ appears as a peak in the $\pi\pi$ mass distribution in D^+ decay, as it does in D_s decay, shows that for the S-wave component the $s\bar{s}$ contribution dominates [16]. Comparing the relative S-wave fit fractions that we observe for D_s^+ and D^+ reinforces this picture. The S-wave decay fraction for the D_s^+ (87%) is larger than that for the D^+ (56%). Rather than coupling to an S-wave dipion, the $d\bar{d}$ piece prefers to couple to a vector state like $\rho^0(770)$ that alone accounts for $\sim$ 30 % of D^+ decay. This interpretation also bears on the role of the annihilation diagram in the $D_s^+ \to \pi^+\pi^-\pi^+$ decay. This study suggests that the S-wave annihilation contribution is negligible over much of the dipion mass spectrum. It might be interesting to search for annihilation contributions in higher spin channels, such as $\rho^0(1450)\pi$ and $f_2(1270)\pi$.

3 Conclusions

Dedicated studies of charm physics are foreseen in the near future at existing collider facilities such as CLEO-c, the B-factories, and the Tevatron. Other facilities might also play a role, such as GSI and Super B-factories. In parallel, the mature stage of the ongoing analysis is providing warnings and lessons on how to perform proper studies to interpret and understand Heavy Flavor phenomenology and, hopefully, to find signs of New Physics.

References

[1] A. J. Schwartz, Mod. Phys. Lett. **A8** (1993) 967.

[2] I. I. Y. Bigi and A. I. Sanda, e-print archive: hep-ph/9909479.

[3] G. Burdman and I. Shipsey, Ann. Rev. of Nucl. and Part. Sci., **53** (2003).

[4] R. Godang *et al.*, Phys. Rev. Lett. **84** (2000) 5038.

[5] S. Bianco, F. L. Fabbri, D. Benson and I. Bigi, Riv. Nuovo Cim., **26N7-8** (2003) 1 .

[6] J. Link *et al.*, Proc. of the 31st. Int. Conf. on High Energy Physics, presented by S. Malvezzi, Nucl. Phys. B Proc. Suppl. **117** (2003) 636.

[7] D.M Asner *et al.* hep-ex/0311033

[8] J. Link *et al.*, Phys. Lett. **B572** (2003) 21.

[9] e-print archive: hep-ex/0405059.

[10] J. Link *et al.*, Phys. Lett. **B535** (2002) 43.

[11] D. Kim for the FOCUS collaboration *Proc. of the XXXVIIIth Rencontres de Moriond, QCD amd High Energy Hadronic Interactions* Les Arcs , March, 2003, also hep-ex/0305038.

[12] J. Link *et al.*, Phys. Lett. **B544** (2002) 89.

[13] J. Link *et al.*, Phys. Lett. **B541** (2002) 243.

[14] J. Link *et al.*, Phys. Lett. **B586** (2004) 283.

[15] S. Spanier and N. A. Törnqvist, Scalar Mesons (rev.), Particle Data Group, Phys. Rev. **D66** (2002) 010001-450.

[16] M. R. Pennington, *Proc. of Oxford Conf. in honour of R. H. Dalitz*, Oxford, July, 1990, Ed. by I. J. R. Aitchison, *et al.,* (World Scientific) pp. 66–107; *Proc. of Workshop on Hadron Spectroscopy* (WHS 99), Rome, March 1999, Ed. by T. Bressani *et al.,* (INFN, Frascati).

[17] E. van Beveren *et al.,* Z. Phys. **C30** (1986) 615.

[18] E. P. Wigner, Phys. Rev. **70** (1946) 15.

[19] S. U. Chung *et al.,* Ann. Physik **4** (1995) 404.

[20] I. J. R. Aitchison, Nucl. Phys. **A189** (1972) 417.

[21] K. L. Au, D. Morgan, and M. R. Pennington, Phys. Rev. **D35** (1987) 1633.

[22] V. V. Anisovich and A. V. Sarantsev, Eur. Phys. J. **A16** (2003) 229.

[23] P. L. Frabetti *et al.,* Phys. Lett. **B407** (1997) 79.

[24] J. Link *et al.,* Phys. Lett. **B585** (2004) 200.

[25] S. Malvezzi *Proc. of the Workshop on Scalar Mesons*, Utica, May, 2003, Ed. by A. H. Fariborz , AIP Conf. Proc. 688, 276, Nucl. Phys. Proc. Suppl. **126**, (2004) 220 also hep-ex/0307055 .

[26] E. M. Aitala *et al.,* Phys. Rev. Lett. **86** (2001) 770.